3ο Πανελλήνιο Συνέδριο Αντισεισμικής
Μηχανικής & Τεχνικής Σεισμολογίας
5–7 Νοεμβρίου, 2008
Άρθρο 1800

A SIMPLIFIED METHOD OF ANALYSIS OF THE SEISMIC RESPONSE OF SLOPES

Sarada K. SARMA–A[1] **, Angelos-Kanellos IRAKLEIDIS–B**[2]

ΠΕΡΙΛΗΨΗ: Σκοπός του παρακάτω άρθρου είναι η παρουσίαση μιας απλοποιημένης μεθόδου ανάλυσης της σεισμικής απόκρισης των πρανών. Κατά την πρόσπτωση κατακόρυφων διατμητικών ημιτονοειδών κυμάτων στην κεκλιμένη εδαφική επιφάνεια, για να ικανοποιηθούν κατά την ανάκλαση οι απαιτήσεις της ισορροπίας και του συμβιβαστού των παραμορφώσεων, παράγονται νέα διαμήκη και διατμητικά κύματα. Αυτό έχει σαν αποτέλεσμα τα ανακλώμενα μαζί με τα προσπίπτοντα κύματα να συνδυάζονται μεταξύ τους εντός της περιοχής του πρανούς, ορίζοντας διάφορες ζώνες απόκρισης. Η σωματιδιακή κίνηση σε κάθε σημείο μπορεί να προσδιοριστεί πλήρως αναλυτικά. Γίνεται η παραδοχή τόξων κύκλου για τις γωνίες ανάμεσα στις οριζόντιες επιφάνειες και την κεκλιμένη επιφάνεια του πρανούς. Η μέθοδος περιορίζεται σε πρανή από ομογενές εδαφικό υλικό, με ελαστικές ιδιότητες και μικρές γωνίες πρανούς. Παρόλο που οι σύγχρονες μέθοδοι ανάλυσης – κύρια η μέθοδος των Πεπερασμένων Στοιχείων ή των Πεπερασμένων Διαφορών κλπ. – μπορούν να μοντελοποιήσουν πολύπλοκες γεωμετρίες και εδαφικές ιδιότητες, η παρουσιαζόμενη μέθοδος μπορεί να αποδειχθεί χρήσιμη για τον έλεγχο των πιο εξεζητημένων μεθόδων, καθώς πρόκειται για μια κλειστή αναλυτική λύση.

ABSTRACT: The aim of this paper is to present a simplified method of analysis of the response of slopes to earthquakes. Vertically propagating shear waves of sinusoidal form are reflected on the sloping ground surface and in order to fulfil the equilibrium and compatibility conditions, shear and longitudinal waves are produced. As a result, these reflected and the incident waves are combined together and different response zones within the slope's area can be defined. The particle motion at every point can be fully defined analytically. An arc of a circle is assumed to connect the horizontal and the sloping surfaces. The method is limited to slopes that are homogeneous, with linear elastic material properties and small sloping angles. Although today's methods of analysis – mostly the Finite Element method, the Finite Difference etc. – are able to model very complex slope geometries and material properties, the presented method may prove useful for the calibration of more sophisticated methods, as it is a closed form solution.

INTRODUCTION

[1] Emeritus Reader, Civil Engineering, Imperial College London, email: s.sarma@imperial.ac.uk
[2] Civil Engineer, MSc DIC, email: airakleidis@tee.gr

When a shear (SV – vertical plane movement) or a compressional (P) wave that travels within an elastic medium reaches the free surface having an angle to the normal to the surface, in order to fulfil the requirements of equilibrium and compatibility at the surface, both SV and P waves are produced. This means that the energy carried by the incident wave is distributed into two new waves, travelling in different directions. After assessing the energy distribution mechanism, which relates to the ratio of the shear-wave and compressional-wave elastic velocities and the angle of incidence, the case of a simple slope is studied. We assume that a vertically propagating shear-wave arrives at a certain depth below the surface at time t=0 and on reaching the free inclined ground surface, the reflections produce SV and P waves at different times. The combination of the reflected waves with the incident waves define areas within the slope, producing complex motions.

REFLECTION OF INCLINED PLANE WAVES ON THE FREE SURFACE

Generally

In figure 1 the cases of the inclined reflection of a SV and a P-wave on the free ground surface is shown.

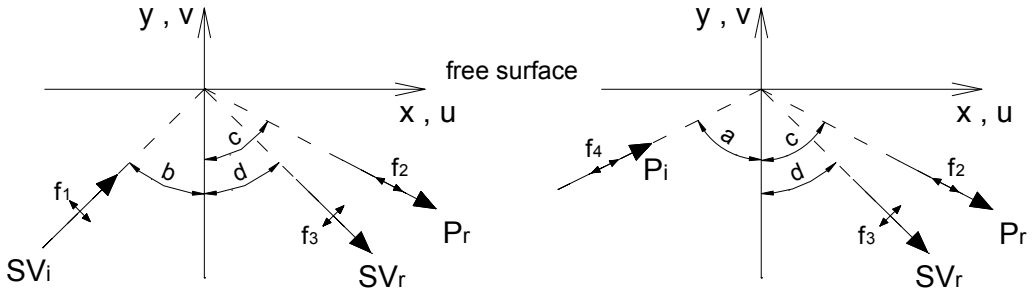

Figure 1. Reflected rays resulting from incident SV and P waves

The direction of the reflected waves is related to the direction of the incident waves, according to the Snell's law:

$$\frac{\sin a}{U} = \frac{\sin b}{V} = \frac{\sin c}{U} = \frac{\sin d}{V} \qquad (1)$$

In table 1 below is shown the notation used. It is the same notation used by Richter (1958):

Table 1. Notation used in the present paper

Wave type	Velocity	Amplitude	Angle with Normal

Incident P	U	A	a
Incident S	V	B	b
Reflected P	U	C	c
Reflected S	V	D	d

In the case of the reflection of the incident SV-wave, the reflected P-wave may graze the free ground surface. This condition determines a critical angle of incidence for the incident SV-wave:

$$b_{cr} = \sin^{-1}\left(\frac{V}{U}\right) \tag{2}$$

In the case of an incident P-wave, there is no critical angle of incidence and the angle can be as much as 90°.

An analysis for harmonic incident waves is studied here, which however can be extended reasonably through Fourier analysis to more complex waves and pulses.

SV incident wave

The energy of the incident SV_i harmonic wave is distributed into the reflected waves SV_r and P_r. Each wave is described with the following expressions:

$$SV_i \Rightarrow f_1 = B \cdot \sin\omega(t - \frac{x \cdot \sin b + y \cdot \cos b}{V}) \tag{3}$$

$$\mathrm{P_r} \Rightarrow f_2 = C \cdot \sin\omega(t - \frac{x \cdot \sin c - y \cdot \cos c}{U}) \tag{4}$$

$$SV_r \Rightarrow f_3 = D \cdot \sin\omega(t - \frac{x \cdot \sin d - y \cdot \cos d}{V}) \tag{5}$$

By expressing the elastic normal stress σ and shear stress τ at the free surface using the above wave equations and placing σ =τ =0, the following expressions are produced for C/B=κ and D/B=λ:

$$\kappa = \frac{\sin 4b}{\frac{V}{U} \cdot \sin 2b \cdot \sin 2c + \frac{U}{V} \cdot \cos^2 2b} \tag{6}$$

$$\lambda = \frac{-\frac{V}{U} \cdot \sin 2b \cdot \sin 2c + \frac{U}{V} \cdot \cos^2 2b}{\frac{V}{U} \cdot \sin 2b \cdot \sin 2c + \frac{U}{V} \cdot \cos^2 2b} \tag{7}$$

P incident wave

The procedure for the calculation of the distribution of the energy of an incident P-wave is similar. The incident P-wave is described with the following expression:

$$P_i \Rightarrow f_4 = A \cdot \sin \omega (t - \frac{x \cdot \sin a + y \cdot \cos a}{U}) \tag{8}$$

If C/A is called μ and D/A=v, the following expressions are worked out:

$$\mu = \frac{\frac{V}{U} \cdot \sin 2a \cdot \sin 2d - \frac{U}{V} \cdot \cos^2 2d}{\frac{V}{U} \cdot \sin 2a \cdot \sin 2d + \frac{U}{V} \cdot \cos^2 2d} \tag{9}$$

$$\nu = \frac{2 \cdot \sin 2a \cdot \cos 2d}{\frac{V}{U} \cdot \sin 2a \cdot \sin 2d + \frac{U}{V} \cdot \cos^2 2d} \tag{10}$$

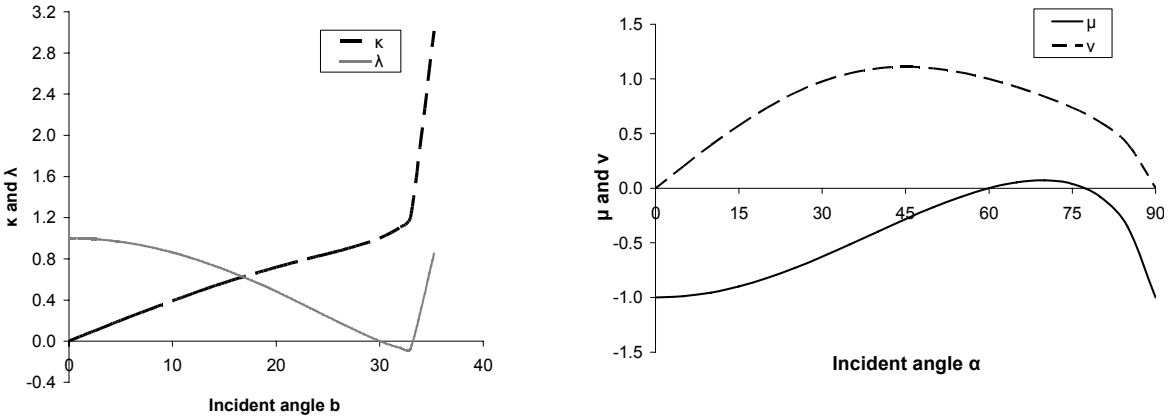

Figure 2: The values of κ,λ,μ and ν vs. the incident angle for a typical ratio U/V=√3

WAVE PROPAGATION ANALYSIS AS APPLIED TO SLOPES

The results presented above are then used for the treatment of the problem of seismic response of slopes. When vertically propagating SV-waves initiate at the same time from a certain depth below the surface (a datum line at depth y=-h in figure 6), they reach the free surface at different times. The inclined incidence of the shear waves, as stated above, generates shear and compressional waves that travel in different directions within the plane. The arrival times of these waves at any point inside the slope will be different. The loss of energy due to the distances travelled by the different waves causing reduction in amplitude of ground motion will also be different. Therefore, every point (x,y) on the plane becomes the junction of waves, the combination of which produces a total particle motion, which is complex.

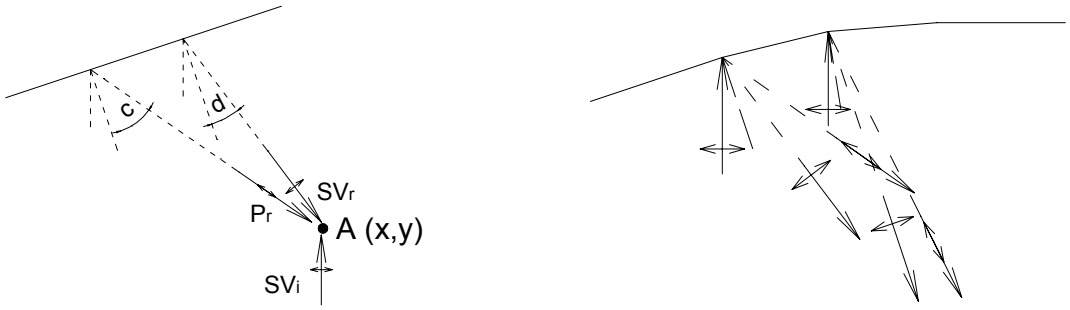

Figure 3: Point A is the junction of three waves, a vertically propagating incident SV, and two reflected waves; a P and a SV from two different points on the free surface. At the second image, when SV-waves reach the arc, there appears dispersion of waves. Note that angle d equals angle b.

Assumption for the corner points

In order to derive a full solution for the whole slope area, an assumption is required for the corner points between the horizontal and the sloping ground, from which there will be dispersion of waves. The simplest assumption that can be made is to assume a very small arc of a circle joining the two lines, which will permit the use of ray theory.

As shown in figure 3 above, the reflected waves depended on the point of the arc where the incident wave hits and therefore will disperse within certain limits. For the reflected SV-waves the limits are between 0 and 2b degrees to the vertical and for the reflected P-wave between zero and (b+c) degrees. However, in the present study, we assume that (b+c) is not bigger than 90 degrees, otherwise a reflected P-wave from the arc will travel along the horizontal free surface. Therefore this is a limiting condition for the method. Also b must be smaller than the critical.

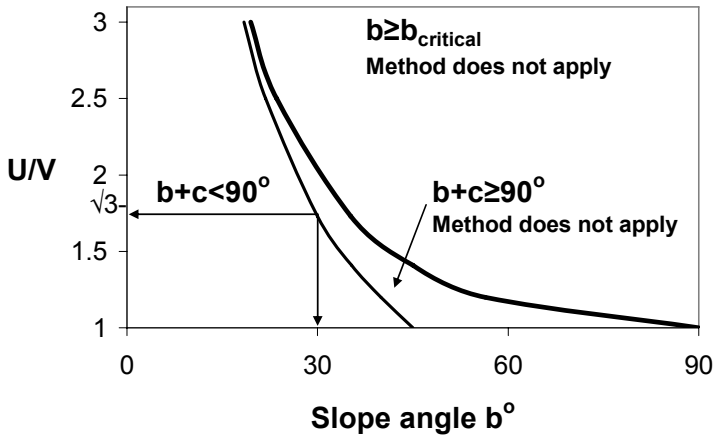

Figure 4: The field of application of the method

Other assumptions

For the analysis, a number of other assumptions are made. These assumptions are about slope geometry, material properties and the incident motion.

The geometry of the slope follows the definition shown in figure 6. Plane strain conditions apply.

The waves travel within a visco-elastic and homogenous medium. No velocity contrast boundary is met within the area of the slope. The loss of energy, which causes reduction to the amplitude of the waves, depends on the ratio of the material damping to the critical, ξ, the frequency of the waves, ω, and the travel time t of the waves within the medium. These are taken into account with a multiplier of exp (-ξ ω t) in the wave equations to the amplitude of motions.

Time is measured from a datum line at a depth y=-h, h>0 (figure 6). All incident SV-waves travel vertically and pass through the datum line at the same time.

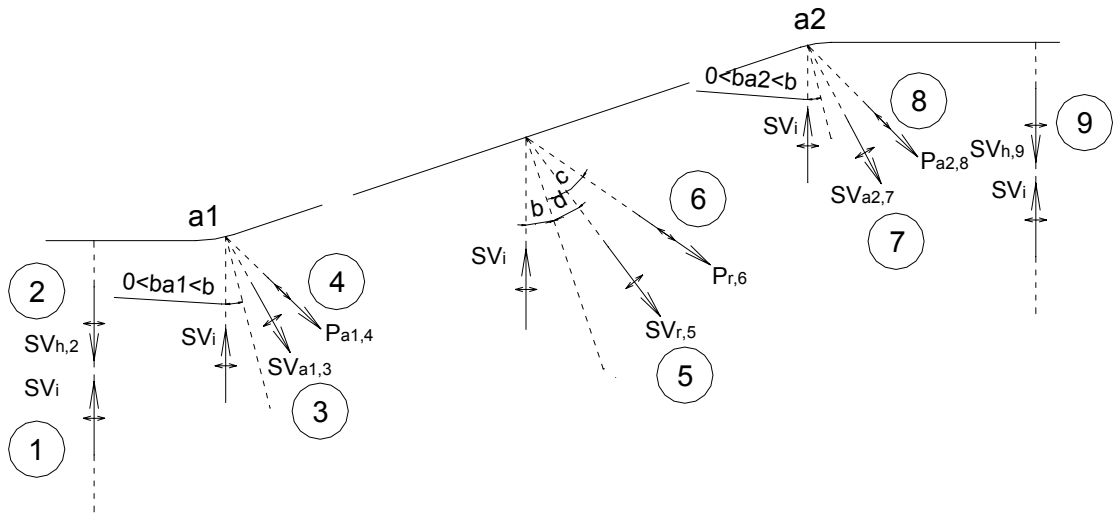

Figure 5. The various wave-types appearing within the slope area

Wave equations

Based on the above definitions and assumptions, the equations of the particle motion for every point in the slope area is calculated as the sum of the motion of the respective waves that pass through this point. According to figure 5, there are nine types of waves that appear in the slope area. Their equations of motion, analysed in two vertical directions – movement on x-axis is represented as u and on y-axis as v – are given next.

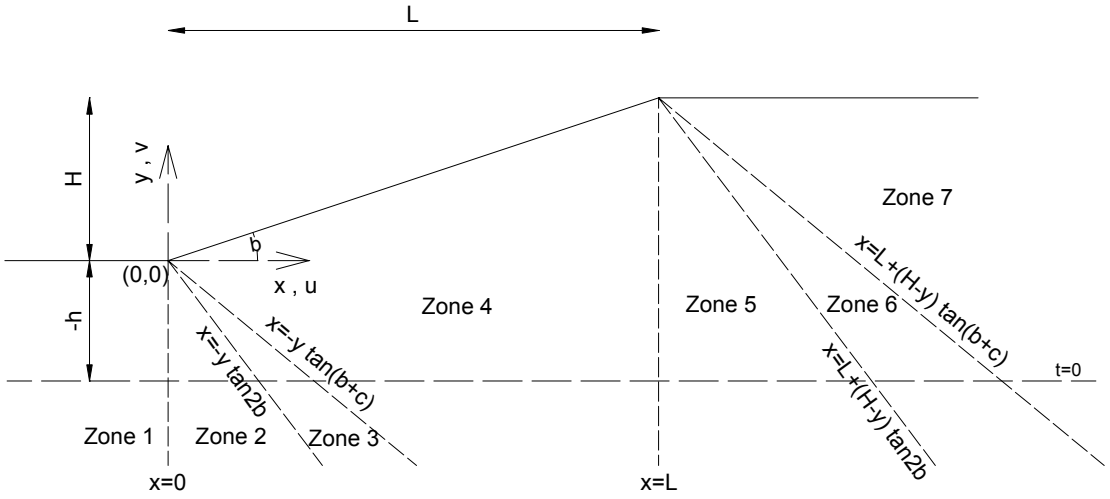

Figure 6. Definition of slope geometry and zoning within the slope area

WAVE 1: Incident SV waves (SV_i)

$$u = B\cdot\sin\omega\left(t-\frac{h+y}{V}\right)\cdot\exp\left(-\xi\cdot\omega\cdot\frac{h+y}{V}\right) \text{ and}$$

$$v = 0$$

Motion at (x,y) initiates at $t \geq \frac{h+y}{V}$

WAVE 2: Reflected SV wave on the horizontal boundary at y=0 ($SV_{h,2}$), x<0

$$u = B\cdot\sin\omega\left(t-\frac{h-y}{V}\right)\cdot\exp\left(-\xi\cdot\omega\cdot\frac{h-y}{V}\right) \text{ and } v = 0$$

Motion at (x,y) initiates at $t \geq \frac{h-y}{V}$

WAVE 3: Reflected SV wave from the arc a_1 ($SV_{a1,3}$)

$$u = \lambda_{a1,S}\cdot B\cdot\sin\omega\left(t-\frac{h+d_{a1,S}}{V}\right)\cdot\cos\left(2b_{a1,S}\right)\cdot\exp\left(-\xi\cdot\omega\cdot\frac{h+d_{a1,S}}{V}\right) \text{and}$$

$$v = \lambda_{a1,S}\cdot B\cdot\sin\omega\left(t-\frac{h+d_{a1,S}}{V}\right)\cdot\sin\left(2b_{a1,S}\right)\cdot\exp\left(-\xi\cdot\omega\cdot\frac{h+d_{a1,S}}{V}\right),$$

It is $d_{a1,S} = -\frac{y}{\cos 2b_{a1,S}}$ and

$$b_{a1,S} = \frac{1}{2}\cdot\arctan\left(\frac{x}{y}\right) \text{and } c_{a1,S} = \sin^{-1}\left(\frac{U}{V}\cdot\sin b_{a1,S}\right)$$

Then $\lambda_{a1,S} = f\left(b_{a1,S}, \frac{U}{V}\right)$

Motion at (x,y) initiates at $t \geq \frac{h + d_{a1,S}}{V}$

WAVE 4: Reflected P-wave from the arc a_1 ($P_{a1,4}$)

$$u = \kappa_{a1,P} \cdot B \cdot \sin\omega\left(t - \frac{h}{V} - \frac{d_{a1,P}}{U}\right) \cdot \sin\left(b_{a1,P} + c_{a1,P}\right) \cdot \exp\left(-\xi \cdot \omega \cdot \left(\frac{h}{V} + \frac{d_{a1,P}}{U}\right)\right) \text{ and}$$

$$v = \kappa_{a1,P} \cdot B \cdot \sin\omega\left(t - \frac{h}{V} - \frac{d_{a1,P}}{U}\right) \cdot \cos\left(b_{a1,P} + c_{a1,P}\right) \cdot \exp\left(-\xi \cdot \omega \cdot \left(\frac{h}{V} + \frac{d_{a1,P}}{U}\right)\right)$$

It is $d_{a1,P} = \frac{-y}{\cos\left(b_{a1,P} + c_{a1,P}\right)}$ and

$$\beta_{a1,P} = b_{a1,P} + c_{a1,P} = \arctan\left(\frac{x}{y}\right) \text{ and } b_{a1,P} = \arctan\left(\frac{V \cdot \sin\left(\beta_{a1,P}\right)}{V \cdot \cos\left(\beta_{a1,P}\right) + U}\right)$$

$$\kappa_{a1,P} = f\left(b_{a1,P}, \frac{U}{V}\right)$$

Motion at (x,y) initiates at $t \geq \frac{h}{V} + \frac{d_{a1,P}}{U}$

WAVE 5: Reflected SV wave on the slope surface ($SV_{r,5}$)

$$u = \lambda \cdot \mathrm{B} \cdot \sin\omega\left(t - \frac{h + h_s + d_s}{V}\right) \cdot \cos 2b \cdot \exp\left(-\xi \cdot \omega \cdot \frac{h + h_s + d_s}{V}\right) \text{ and}$$

$$v = \lambda \cdot B \cdot \sin\omega\left(t - \frac{h + h_s + d_s}{V}\right) \cdot \sin 2b \cdot \exp\left(-\xi \cdot \omega \cdot \frac{h + h_s + d_s}{V}\right), \text{ where}$$

$$d_s = \frac{x - x_s}{\sin 2b}, \; h_s = x_s \cdot \tan b \text{ and } x_s = \frac{x + y \cdot \tan 2b}{1 + \tan b \cdot \tan 2b}$$

Motion at (x,y) initiates at $t \geq \frac{h + h_s + d_s}{V}$

WAVE 6: Reflected P-wave on the slope surface ($P_{r,6}$)

$$u = \kappa \cdot B \cdot \sin\omega\left(t - \frac{h + h_P}{V} - \frac{d_P}{U}\right) \cdot \sin\left(b + c\right) \cdot \exp\left(-\xi \cdot \omega \cdot \left(\frac{h + h_P}{V} + \frac{d_P}{U}\right)\right) \text{ and}$$

$$v = \kappa \cdot B \cdot \sin\omega\left(t - \frac{h + h_P}{V} - \frac{d_P}{U}\right) \cdot \cos\left(b + c\right) \cdot \exp\left(-\xi \cdot \omega \cdot \left(\frac{h + h_P}{V} + \frac{d_P}{U}\right)\right), \text{ where}$$

$$d_P = \frac{x - x_P}{\sin(b + c)}, h_P = x_P \cdot \tan b \text{ and } x_P = \frac{x + y \cdot \tan(b + c)}{1 + \tan b \cdot \tan(b + c)}$$

Movement at (x,y) initiates at $t \geq \frac{h + h_P}{V} + \frac{d_P}{U}$

WAVE 7: Reflected SV wave from the arc a_2 ($SV_{a2,7}$)

$$u = \lambda_{a2,S} \cdot B \cdot \sin\omega\left(t - \frac{h+H+d_{a2,S}}{V}\right) \cdot \cos\left(2b_{a2,S}\right) \cdot \exp\left(-\xi \cdot \omega \cdot \frac{h+H+d_{a2,S}}{V}\right) \text{ and}$$

$$v = \lambda_{a2,S} \cdot B \cdot \sin\omega\left(t - \frac{h+H+d_{a2,S}}{V}\right) \cdot \sin\left(2b_{a2,S}\right) \cdot \exp\left(-\xi \cdot \omega \cdot \frac{h+H+d_{a2,S}}{V}\right)$$

It is $d_{a2,S} = \dfrac{H-y}{\cos\left(2b_{a2,S}\right)}$,

$b_{a2,S} = \dfrac{1}{2} \cdot \arctan\left(\dfrac{x-L}{H-y}\right)$ and $c_{a2,S} = \sin^{-1}\left(\dfrac{U}{V} \cdot \sin b_{a2,S}\right)$

and $\lambda_{a2,S} = f\left(b_{a2,S}, \dfrac{U}{V}\right)$

Motion at (x,y) initiates at $t \geq \dfrac{h+H+d_{a2,S}}{V}$

WAVE 8: Reflected P wave from the arc a_2 ($P_{a2,8}$)

$$u = \kappa_{a2,P} \cdot \mathrm{B} \cdot \sin\omega\left(t - \frac{h+\mathrm{H}}{V} - \frac{d_{a2,P}}{U}\right) \cdot \sin\left(b_{a2,P} + c_{a2,P}\right) \cdot \exp\left(-\xi \cdot \omega \cdot \left(\frac{h+\mathrm{H}}{V} + \frac{d_{a2,P}}{U}\right)\right) \text{ and}$$

$$v = \kappa_{a2,P} \cdot \mathrm{B} \cdot \sin\omega\left(t - \frac{h+\mathrm{H}}{V} - \frac{d_{a2,P}}{U}\right) \cdot \cos\left(b_{a2,P} + c_{a2,P}\right) \cdot \exp\left(-\xi \cdot \omega \cdot \left(\frac{h+\mathrm{H}}{V} + \frac{d_{a2,P}}{U}\right)\right)$$

It is $d_{a2,P} = \dfrac{H-y}{\cos\left(b_{a2,P} + c_{a2,P}\right)}$

$\beta_{a2,P} = b_{a2,P} + c_{a2,P} = \arctan\left(\dfrac{x-L}{H-y}\right)$ and $b_{a2,P} = \arctan\left(\dfrac{V \cdot \sin\left(\beta_{a2,P}\right)}{V \cdot \cos\left(\beta_{a2,P}\right) + U}\right)$

Then $\kappa_{a2,P} = f\left(b_{a2,P}, \dfrac{U}{V}\right)$

Motion at (x,y) initiates when $t \geq \dfrac{h+H}{V} + \dfrac{d_{a2,P}}{U}$

WAVE 9: Reflected SV wave on the horizontal boundary at y=H ($SV_{h,9}$), x>H cot b

$$u = B \cdot \sin\omega\left(t - \frac{h+2H-y}{V}\right) \cdot \exp\left(-\xi \cdot \omega \cdot \frac{h+2H-y}{V}\right) \text{ and } v = 0\,.$$

Motion at (x,y) initiates when $t \geq \dfrac{h+2H-y}{V}$

Division to zones

According to figure 6, the slope area can be divided to seven zones, within which different combinations of waves appear. The limits of the zones are given in the figure as well. The combination of waves that pass through every zone is shown in table 2.

Table 2. The wave-types present in every zone of the slope

Zone	SV_i	$SV_{h,1}$	$SV_{a1,3}$	$P_{a1,4}$	$SV_{r,5}$	$P_{r,6}$	$SV_{a2,7}$	$P_{a2,8}$	$SV_{h,9}$
1	√	√							
2	√		√	√					
3	√			√	√				
4	√				√	√			
5	√				√	√	√	√	√
6	√					√		√	√
7	√								√

Application of the method

Based on the above, e.g. the horizontal displacements for any point (x,y) within zone 3 are calculated as:

$$u = B\cdot\sin\omega\left(t-\frac{h+y}{V}\right)\cdot\exp\left(-\xi\cdot\omega\cdot\frac{h+y}{V}\right)+$$
$$+\kappa_{a1,P}\cdot B\cdot\sin\omega\left(t-\frac{h}{V}-\frac{d_{a1,P}}{U}\right)\cdot\sin\left(b_{a1,P}+c_{a1,P}\right)\cdot\exp\left(-\xi\cdot\omega\cdot\left(\frac{h}{V}+\frac{d_{a1,P}}{U}\right)\right)+$$
$$+\lambda\cdot\mathrm{B}\cdot\sin\omega\left(t-\frac{h+h_s+d_s}{V}\right)\cdot\cos 2b\cdot\exp\left(-\xi\cdot\omega\cdot\frac{h+h_s+d_s}{V}\right)$$

Then the method is applied to a slope with the following characteristics; L=300 m, H =100m, U/V=√3 (say U=520 m/s and V=300 m/s) and material damping ξ=0,05. The datum of t=0 is set at y=0. The incident sinusoidal wave, with B=1,0 m and ω=2π rad/s, is expressed as:

$$u=\sin 2\cdot\pi\left(t-\frac{y}{300}\right)\cdot\exp\left(-\frac{y}{3000}\right)\ \text{and}\ v=0$$

The following graphs (figure 7) show the response of different points at the surface of the slope. The difference at arrival times is clearly illustrated and the loss of energy – different at each point – due to damping as well. Horizontal and vertical motions appear at the slope's surface. In figure 8 the motion at various points at the slope's area are presented.

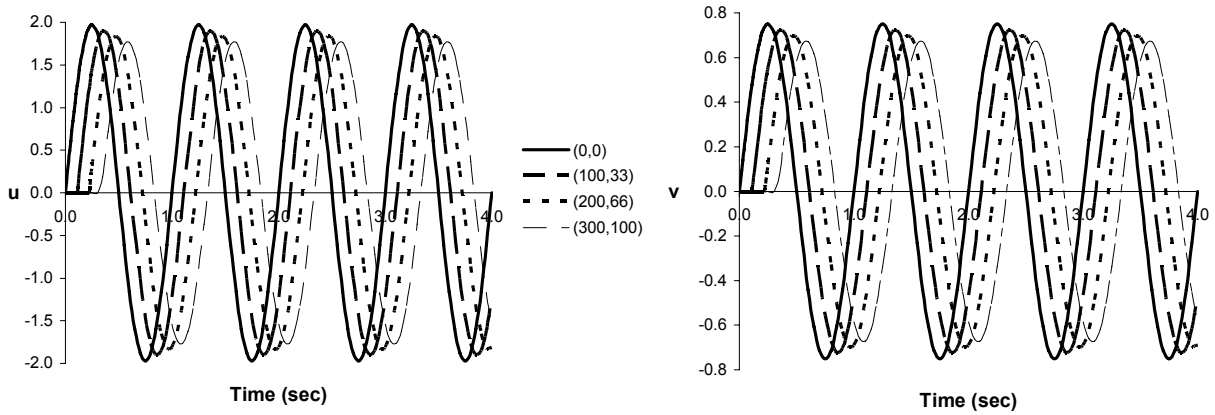

Figure 7. Horizontal and vertical motion at various points of the free surface

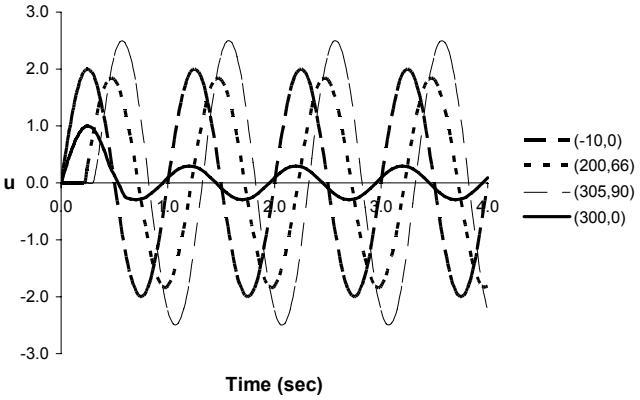

Figure 8. The horizontal motion of two points within the slope's area and two points at the surface. The arrival of the reflected waves may increase or reduce the initial motion.

CONCLUSIONS

A wave propagation solution to the slope seismic response problem is given. The procedure is simple and the method is restricted to simple cases that follow a number of assumptions about slope geometry and material properties. However, a closed-form solution is established, which may prove useful for the calibration of complex and sophisticated codes that are often used for the analysis of this kind of problems.

ACKNOWLEDGEMENTS

The work presented above was done in the Imperial College London in the period between March and June 2003, during an exchange program between the latter and the National Technical University of Athens. The second writer would like to express his gratitude to the

Imperial College London for allowing him to work in the Civil and Environmental Engineering Department of the College under the supervision of the first writer and that he was able to make full use of all the essential equipment and services. He is also grateful to the NTUA and especially to Professor A. Anagnostopoulos for allowing him to work his Diploma Thesis in the Imperial College, offering all kinds of support.

REFERENCES

Irakleidis A., (2003), “An investigation on seismic slope stability”, Diploma Thesis, Imperial College London, Department of Civil and Environmental Engineering

Kramer S.L., (1996), “Geotechnical Earthquake Engineering“, Prentice - Hall, Inc., New Jersey

Richter, C.F., (1958), “Elementary Seismology”, W.H. Freeman, San Francisco